Non-contact Ultrasonic Technique for Detection of Initial and Final Set Times of Low-Carbon Cementitious Materials

by Linh Nguyen and Quang Tran

Biography:

ACI member **Linh Nguyen** is a PhD student in the Department of Civil, Environmental, and Geospatial Engineering at the Michigan Technological University (MTU), MI. She received her BS in building materials technology from the National University of Civil Engineering, Vietnam; her MS in Civil Engineering Technology (CET) from SIIT, Thammasat University, Thailand. Her research interests include nondestructive testing of concrete and its application to 3D-printed concrete, as well as low-carbon cement materials.

ACI member **Quang Tran** is an Assistant Professor at Michigan Technological University. He received his PhD degree in Civil Engineering at the University of Illinois at Urbana-Champaign. Dr. Tran dedicated three years to postdoctoral research, contributing his expertise to prestigious institutions including Harvard Medical School, Harvard affiliated hospitals, and the Bioacoustics Research Lab at the University of Illinois at Urbana-Champaign. His research interests span diverse disciplines, encompassing material characterization, nondestructive evaluation (NDE), and advanced sensing technologies, with applications in civil and environmental engineering as well as biomedical challenges.

ABSTRACT/SYNOPSIS

In situ, accurately determining concrete set times is essential for precise scheduling, reducing costs, and ensuring quality during concrete construction. The non-contact ultrasound technique (nUT) offers a modern with high precision, a non-destructive approach, reduced time and labor waste, and is suitable for laboratory and field test settings, overcoming challenges of standard methods. Additionally, the advent of new cementitious materials like LC3 and OPC1L has further complicated the estimation and control of set times in the field. This study investigates the feasibility of using a portable and compact nUT device to precisely determine both initial and final set times of cementitious materials. Six mixtures were prepared using

OPC1L, LC3, and fly ash at two common w/c ratios (0.4 and 0.5) and tested concurrently using Vicat needle measurements. The results demonstrate that nUT effectively identifies both the initial and final times, and Pearson R = 78% between nUT and the initial set times.
Keywords: non-contact ultrasonic technique (nUT); leaky Rayleigh wave (LR wave); low-carbon cement pastes; Vicat initial set times; Vicat final set times.

INTRODUCTION

Accurately determining the set time of concrete is crucial because it directly affects workability, strength, schedule, and long-term durability of construction projects**.** The initial set time of concrete is defined as the time at which the concrete starts to lose its plasticity, while the final setting time is the time at which the concrete begins to form a hardened mass and achieve its maximum hydration heat[1,2]. In a construction project, the initial setting time should not be excessively rapid to ensure sufficient time to complete some processes, such as mixing, transporting, and pouring, before it is finished. Additionally, the final setting time should not be unnecessarily delayed, so subsequent processes can begin sooner. The postponement of successive phases, such as formwork removal and other traffic-related construction activities, results in unnecessary expenditure of time, labor, and financial resources[2]. In pavement construction, the ideal moment to perform the final curing is during the initial setting of the concrete[3]. The final set time influences the timing of saw cutting to prevent random cracking[4]. In 3D concrete printing, the initial setting time is particularly critical, as it governs the material's ability to sustain successive extruded layers without deformation[5].

Standard methods, such as the Vicat testing[6] and penetration resistance[7] test can determine the set times of cementitious materials. However, they have several challenges, including manually operated, labor-intensive, time-consuming, and prone to errors caused by human mistakes subjectivity. These tests must be conducted at various time intervals, particularly when used with rapid-setting mixtures, as interpolation can lead to inaccuracies[8]. A penetration test[7] employs wet sieving to extract the mortar fraction from concrete, which is labor- and time-intensive and produces waste. Additionally, these tests are experiential as they are often operated by operators, which can lead to output inconsistency.

Several ultrasonic alternative techniques have been developed to overcome the difficulties associated with standard methods for determining the set time of cementitious materials. A study [9] applied S-wave ultrasonic wave reflection (UWR) to measure the setting time of cement paste. This test used a 2.25 MHz S-wave transducer in direct contact with the specimen. The signals were recorded at 5-minute intervals during 24 hours of hydration progression and then compared to the penetration resistance test results. The results show that the initial set time of the cement paste is defined when the acoustic impedance reaches 0.09 MRayls, which is only applicable to the HIPS buffer type used in this study. The start of stiffening was identified by analyzing the derivative of the reflection coefficient over time (R(t)). The final set time from the S-wave UWR is determined to be when the dR/dt curve reaches the minimum value[9]. However, the UWR set time results appear strongly dependent on the buffer type, which requires a material with low acoustic impedance. Additionally, it needs to be examined further to confirm that 0.09 MRayls is accurate for other types of samples. The set times obtained using the defined criteria with S-wave UWR data generally agreed but did not match exactly with the values determined through penetration resistance. Another study[10] utilized the UWR technique to investigate the evolution of microstructure in early-age cement paste. This experiment used two shear-wave transducers with frequencies of 2.6 MHz and 4.6 MHz, applying a 400 V pulser-receiver peak square pulse. The paper outcome emphasizes the importance of frequency dependence in determining the initial set time of paste by explaining it through the reflection of transitions in pore connectivity. The critical time of frequency dependence has been strongly correlated with the Vicat testing results[10]. Final set time is also defined by applying the ultrasonic wave reflection direct (UWRD) and the ultrasonic wave reflection indirect (UWRI) methods. A study[8] analyzes the waveform signals of the P-wave (1.0 MHz) and S-wave (2.25 MHz) using the Fast Fourier Transform (FFT) and Short-Time Fourier Transform (STFT) processing. Key findings indicate that both UWRD and UWRI techniques accurately define the final set time of the cement paste when compared to Vicat testing. UWRD determines the final set time via the first arrival of reflected waves (falls within 5% of the Vicat standard), and UWRI specifies the minimum amplitude location in S-wave reflection as the final set time (6% of the Vicat)[8].

Although the UWR method offers many advantages, it still has some limitations when determining the time of cementitious materials. The determination of the initial set time remains challenging due to high attenuation and a significant noise floor while the concrete is still in its liquid state phase[8]. As mentioned above, the absence of applicable standards for selecting buffer materials complicates the process of monitoring the setting behavior when different buffers are employed[8]. Notably, the UWR result is influenced by the inhomogeneity of materials, which includes aggregates and air voids present in the concrete. These factors contribute to the variability and inaccuracy in reflecting the set time results detected by UWR[11].

Besides UWR techniques, another method capable of determining the set time of cementitious materials is ultrasonic pulse velocity (UPV)[12, 13]. A study applied UPV to monitor the set time of ultra-high performance cementitious materials (UHPC) using direct-contact piezoelectric transducers with testing frequency centered at 24.4 kHz. The research results show that the final times of various cementitious materials are very close to the arrival time at the maximum UPV changing rate[14]. However, selecting the transmission time of fresh pastes presents significant challenges, especially before the cementitious materials set. This difficulty arises from the substantial attenuation of ultrasonic waves in plastic cementitious pastes, which causes considerable interference from signal noise. Benaicha et al.[15] demonstrate that varying probe positions will affect the ultrasonic velocity. The direct mode, wherein the transmitter and receiver are positioned directly opposite each other, provides the most reliable measurements. Additionally, using UPV to find the set times relies heavily on the experimenters' interpretation of the results, leading to different outcomes.

Another research study utilized guided waves in a reinforcing bar that went through a concrete beam specimen, as it is known that Ultrasonic Pulse Transmission Testing (UPT) has the potential to monitor the set time. The bar attached is a waveguide that assists in wave propagation. Ultrasonic longitudinal guided waves were applied because they can be easily generated by attaching a transducer at the end of the bar. Two longitudinal (L) ultrasonic modes are used, specifically L (0,1) at 0.1 MHz and L (0,7) at 1 MHz. The amplitude of the received signal (peak-to-peak voltage) is normalized with the initial pause, resulting in parameter R. The sudden change in the slope of the R vs time curve is defined as the initial set time of

concrete. When the R-value levels off and remains steady, the final set time is achieved[16]. The steel used is plain bar, but mostly rib bars are used in the construction site, which will affect energy leakage and might not translate directly from the findings. Additionally, these findings are highly sensitive and significantly depend on the ultrasonic mode; therefore, it is crucial to select the mode and frequency correctly before conducting the project.

Among ultrasound techniques, one of the most advanced methods is non-contact, which utilizes a leaky Rayleigh wave (LR wave) to estimate the final set time of concrete, resulting in successful outcomes. Tran and Roesler[17] developed a non-contact ultrasonic (nUT) system that can quickly determine the final set time of concrete in both laboratory and field conditions without mechanical coupling or embedded sensors by using low-cost contactless sensors (microelectromechanical) and data acquisition systems to detect the LR wave from the concrete surface. The rising point of the LR wave energy versus time curve, defined as the final set time, correlates very well with the penetration test results. Another research utilized nUT to determine the final set time of high-volume fly ash concrete (HVFAC). The final set of times obtained agrees very well with the isothermal calorimetry heat curve results[18]. This result demonstrates that monitoring LR waves can define the exact final set time of different types of concrete, including those containing supplementary cementitious materials (SCMs).

Bai et al.[19] describes a non-contact acoustic emission (AE) localization technique that utilizes leaky Rayleigh waves detected by an innovative air-coupled microelectromechanical systems (MEMS) microphone array. The research demonstrates that this methodology can precisely identify the direction of arrival of the AE source at different positions, with results that closely match the actual coordinates. Rayleigh waves are captured in the air over distances exceeding one meter within an appropriate frequency range of 5-22 kHz.

At present, NDT has not yet succeeded in supplanting the conventional method for ascertaining both the initial and final set times of cementitious materials, despite its advantages. Recognizing this significant gap, this research goal is to accurately measure the initial and final set times of cementitious materials by utilizing nUT, specifically by monitoring the LR wave emitted from the concrete surface during hydration. To attain this objective, six different

mixtures with two distinct w/c ratios of 0.4 and 0.5 were utilized to assess nUT. The use of low-carbon materials, including OPC1L cement and limestone calcined clay cement (LC3), was implemented to mitigate the global carbon footprint problem. Notably, a new, highly practical device has been developed for field applications, enhancing the feasibility and relevance of this method in real-world settings.

THEORY BACKGROUND

A Rayleigh wave (R-wave) is a type of surface wave that consists of both P- and S-waves, and it can occur at the surface of a homogeneous medium[20]. R-wave is the one propagating along the interface and leaking to the air, known as Leaky Rayleigh waves (LR waves). The velocities of longitudinal (c_L) and transverse bulk elastic waves (c_T) and Rayleigh waves (c_R) are shown in Equations (1), (2), and (3), respectively[21].

$$c_L = \sqrt{\frac{E(1-\nu)}{\rho_s(1+\nu)(1-2\nu)}} \quad \text{(Eq. 1)}$$

$$c_T = \sqrt{\frac{E}{2\rho_s(1+\nu)}} \quad \text{(Eq. 2)}$$

$$c_R = 0.9c_T \quad \text{(Eq. 3)}$$

where E is the elastic modulus and ν is Poisson's ratio of a material.

The properties of LR waves reflect the characteristics of the material they travel through[20,22]. Due to this distinctive characteristic, the LR wave is employed to monitor the hydration and stiffening progression of cementitious materials (air-concrete interface). While the concrete remains in a fluid state, it lacks shear resistance; consequently, an LR wave does not propagate along the concrete. As time progresses, hydration reactions are initiated within the concrete, resulting in increased stiffness and a transition from a liquid to a semi-rigid state, ultimately culminating in the formation of a solid phase. During this transition, shear capacity is established, and the R-wave begins propagating along the surface of the concrete, dispersing into the air. Accordingly, the initial observation of LR wave signals can serve as an indicator of the early stiffening and setting process of the concrete material[17, 23, 24].

The critical angle is the incident angle at which waves travel along the surface of a solid without producing any further refracted or reflected waves further into material[23]. To efficiently generate LR wave energy within a particular material, incident waves should be directed at or near this critical angle. The velocity of the LR wave depends on the incident angles, as indicated in Equation (4). It is necessary to adjust the incident angle to effectively detect the LR wave across different velocity levels and varying stiffness conditions (Equations-1, 2, 3, and 4). The critical angle (θc) as calculated in Equation (4), follows Snell's law[4,17, 23].

$$\theta c = \arcsin\left(\frac{343}{\mathrm{Vc}}\right) \quad \text{(Eq. 4)}$$

where Vc is the R-wave velocity (m/s) and 343 (m/s) is the speed of sound in the air. As concrete hydrates, the velocity of the leaky surface wave increases with the bulk modules and density, and the critical angle decreases continuously. Therefore, when measuring the final set time of concrete, the system uses a lower incident angle (e.g., 12 degrees). As the speed of sound of cementitious materails at initial settint time is lower, it is hypothesized to increase the incident angle, such as 20 to 40 degrees[4, 17, 23].

RESEARCH SIGNIFICANCE

Determining both initial and final set times accurately with nUT provides continuous, real-time measurement, enabling rapid estimation of concrete set times in laboratory or field settings without embedded receivers or mechanical coupling. Consequently, contractors can schedule finishing, saw-cutting, and formwork removal based on actual material behavior rather than coarse, intermittent readings. This approach minimizes premature loading, reduces the risk of random cracking, and prevents schedule delays, particularly for low-carbon binders whose setting characteristics may differ from those of tradition mixtures. Producers and researchers are provided with a swift, reproducible method for comparing mixtures and optimizing low-carbon blend designs.

EXPERIMENTAL INVESTIGATION

1. Mix design and test specimens

Six cement paste mixtures comprising low-carbon cement OPC1L, low-carbon limestone calcined clay cement (LC3), and fly ash type F (FA) were used for nUT and standard Vicat

(ASTM C191)[6] tests simultaneously. OPC1L is an innovative material to replace ordinary Portland cement in concrete. OPC1L lowers greenhouse gas (GHG) emissions and reuses industrial byproducts during concrete production as it reduces clinker content in Portland cement[25]. Another innovative material used is LC3, which substitutes a substantial part of traditional clinker with calcined clay and limestone. It can reduce CO_2 emissions by 30–40% compared to ordinary Portland cement, mainly by decreasing clinker content and demanding less energy during clay processing[26]. There are two different w/c ratios, such as 0.4 and 0.5 were used. The proportion of the six mixtures used is shown in Table 1. The specific gravity of OPC1L cement, FA, and LC3 are 3.15, 2.32, and 2.87 g/cm^3, respectively.

Table 1. Paste mixture proportions used in this study (All weights are in pounds/ cubic yards)

Mixture	w/c	Water	Cement	Fly ash	LC3
100OPC1L-04	0.4	228	570	0	0
100OPC1L-05	0.5	285	570	0	0
70OPC1L:30FA-04	0.4	228	400	170	0
70OPC1L:30FA-05	0.5	285	400	170	0
100LC3-04	0.4	228	0	0	570
100LC3-05	0.5	285	0	0	570

Note: Mixture systematically identifies the mixture's composition and w/c. For example, in the mixture 70OPC1L:30FA-04, the 70OPC1L:30FA part denotes a binder blend of 70% OPC1L cement and 30% fly ash by weight, while the -04 suffix indicates a W/C ratio of 0.4.

One prism with 100 x 100 x 400 mm in W×H× L was prepared for each mixture for using the nUT testing. At the same time, a conical ring was used to test the setting time, with a height of 40 mm and an inside diameter of 60 mm at the top and 70 mm at the bottom[6].

2. Standard Vicat test (ASTM C191) to determine the setting times of the paste

The Vicat test specifies a method for determining the initial setting times of paste by measuring the sample's penetration depth at 25 mm. The Vicat time of initial setting is calculated to the nearest 1 minute as Equation (5)[6]:

$$\left(\left(\frac{\mathrm{H}-\mathrm{E}}{C-D}\right)\times(C-25)\right)+E \qquad \text{(Eq. 5)}$$

where E is time in minutes of last penetration greater than 25 mm, H is time in minutes of first penetration less than 25 mm, C is penetration reading at time E, and D is penetration reading at time H.

The Vicat final set time is measured from the initial contact of the cementitious material with water to the point at which the Vicat test indicates final setting. It is marked when the circular impression no longer leaves a complete circle on the sample's surface[6].

3. Experimental setup for nUT

The schematic of the battery nUT device on a beam specimen to monitor the set times is shown in Figure 1. An electrostatic-type ultrasonic transmitter with a 50kHz frequency ultrasonic pulse and a transmission of 16 cycles is used. The transducer is placed inside a mold to reduce air acoustic waves' amplitude. A non-contact receiver features a multi-channel sensing array comprising 16 receivers with a 7mm spacing and placed on the other side of the prism. This ultrasonic receiver includes a pre-amplifier, filter, and signal conditioning circuitry, highlighting one of the advantages of this configuration—its flexibility and compactness design. Between the transmitter and the PCB receiver board, an acoustic baffle is placed to attenuate the direct air acoustic signals from the transmitter and the reflected signal from the mortar surface sample. To streamline the system, a touchscreen display is mounted on a frame to monitor LR wave data signals over time.

All the equipment is housed within a sleek, 3D-printed frame, crafted to maximize the system's adaptability and ease of use in field conditions. This innovative design allows precise control over key parameters, such as the incident angle and the distance from the transmitter to sensors and from sensors to the surface sample. As shown in Figure 2, the system is a custom creation by portable and compact nUT. This setup shows potential to revolutionize field measurements with its ingenuity and practicality.

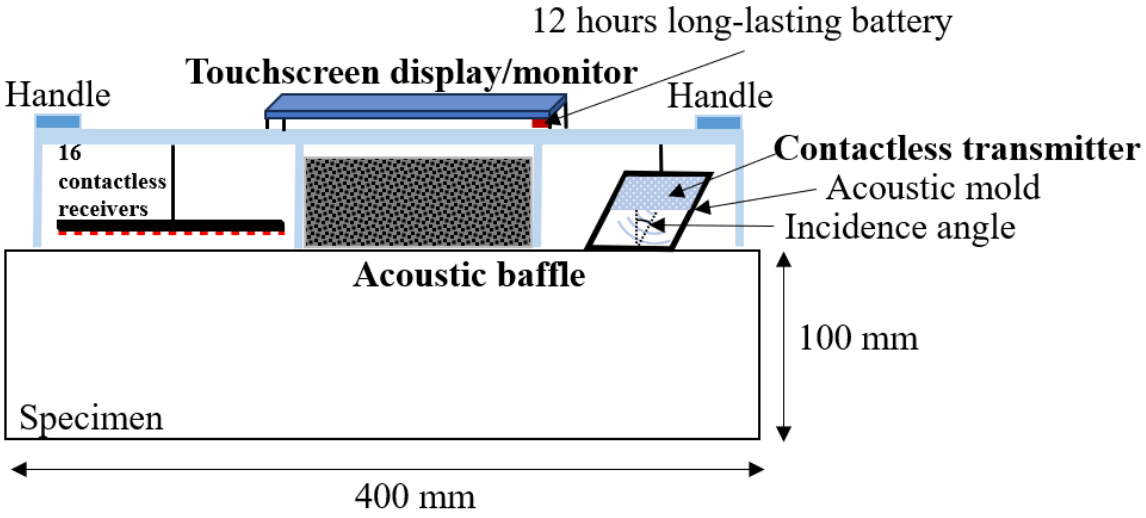

Figure 1. Schematic diagram of the nUT system testing employed in this research

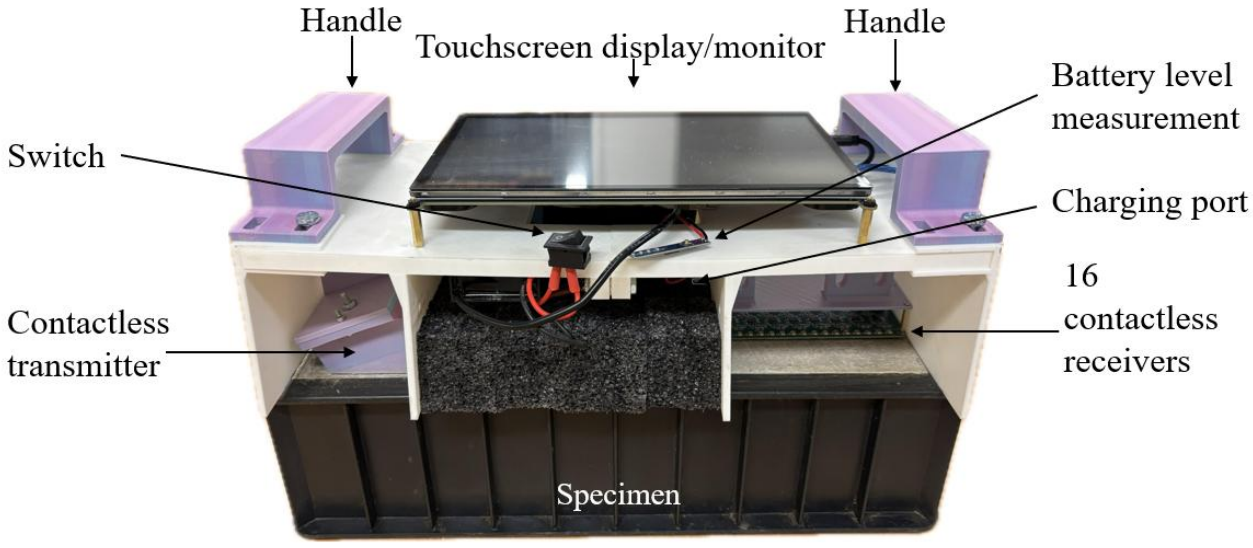

Figure 2. Real image of portable and compact nUT system.

ANALYTICAL INVESTIGATION

To enhance the generalizability, consistency, and accuracy of the technique, a novel signal-processing algorithm uses sensor outputs to determine the LR wave energy and correlates it with the standard Vicat set times. The following steps outline the signal processing and analysis procedure following data acquisition.

Step 1 – Load Data and Configure Temporal and Spatial Axes: Filtered ultrasonic signals were obtained from an array of 16 channels. The dataset was imported into MATLAB for post processing.

Step 2 – Select a Channel and Remove Direct Arrival: A representative channel was chosen, and direct acoustic arrivals were eliminated using an automated detection algorithm. This routine identified the noise-arrival boundary and the direct acoustic arrival, enabling the waveform to be truncated to retain only the LR wave signals.

Step 3 – Generate 2D Heatmap for Multiple Acquisitions of Selected Channel: The truncated signals were assembled into a 2D matrix representing material age versus wave-propagation time. A custom heatmap routine mapped signal amplitudes onto this time-age domain, thereby producing a development curve illustrating the temporal evolution of the LR wave as the cementitious material transitioned from fluid to semi-solid. Variations in wave coherence, amplitude growth, and wavefront clarity were evident in the heatmap.

Step 4 - Overlay Vicat Initial and Final Set Times: These times were superimposed on the plot to facilitate comparison between the standard method and the nUT. The final heatmap and annotations were archived for subsequent interpretation and reporting.

COMPARISON OF PREDICTIONS AND EXPERIMENTAL RESULTS

From a theoretical perspective, LR waves become measurable only when cementitious materials attain sufficient stiffness and shear capacity, signifying the transition from liquid to solid states. Consequently, the initiation and amplitude growth of LR wave signals serve as dependable indicators of both the initial and final set times. The hypothesis is that nUT can detect the initial and final set times of materials. The results obtained will correlate well with the standard method.

Importantly, the selection of the incident angle is not random: during early hydration stages, higher angles are needed to excite LR wave in low-stiffness media, while as stiffness increases, lower incident angles improve LR wave detection and signal quality. Therefore, the hypothesis is that nUT can identify the initial and final set times of materials by adjusting incident angles.

EXPERIMENTAL RESULTS AND DISCUSSION

1. Effect of incident angles on LR wave

Figure 3 illustrates the evolution of LR wave response at three incident angles (20, 25, and 30 degrees) as a function of material age. The Vicat initial and final set times are superimposed for comparison, at 560 and 875 minutes, respectively. Two wave patterns are identified: leaky Rayleigh (LR) and direct acoustic (DA) waves. The LR wave appears as a curved band of relative low amplitude and shifts toward shorter capture times as the material stiffens. DA wave forms a strong, nearly vertical high amplitude, and parallel arrival.

Previous research by Tran and Roesler[17] demonstrated that incident angles below 30 degrees effectively excite the LR wave with a velocity exceeding that of the direct acoustic wave. However, if the angle of incidence is too small, the initial phases of stiffening and setting processes may be neglected[23]. In this study, the incident angles detect the LR wave signals before the initial set time of cement pastes were evaluated. At 20 degrees, the LR wave initiates significantly earlier compared to Vicat initial set times, with signal emergence at 363 minutes. As the incident angle increases to 25 and 30 degrees, the signal starts later, appearing at 538 and 673 minutes (see Figure 3).

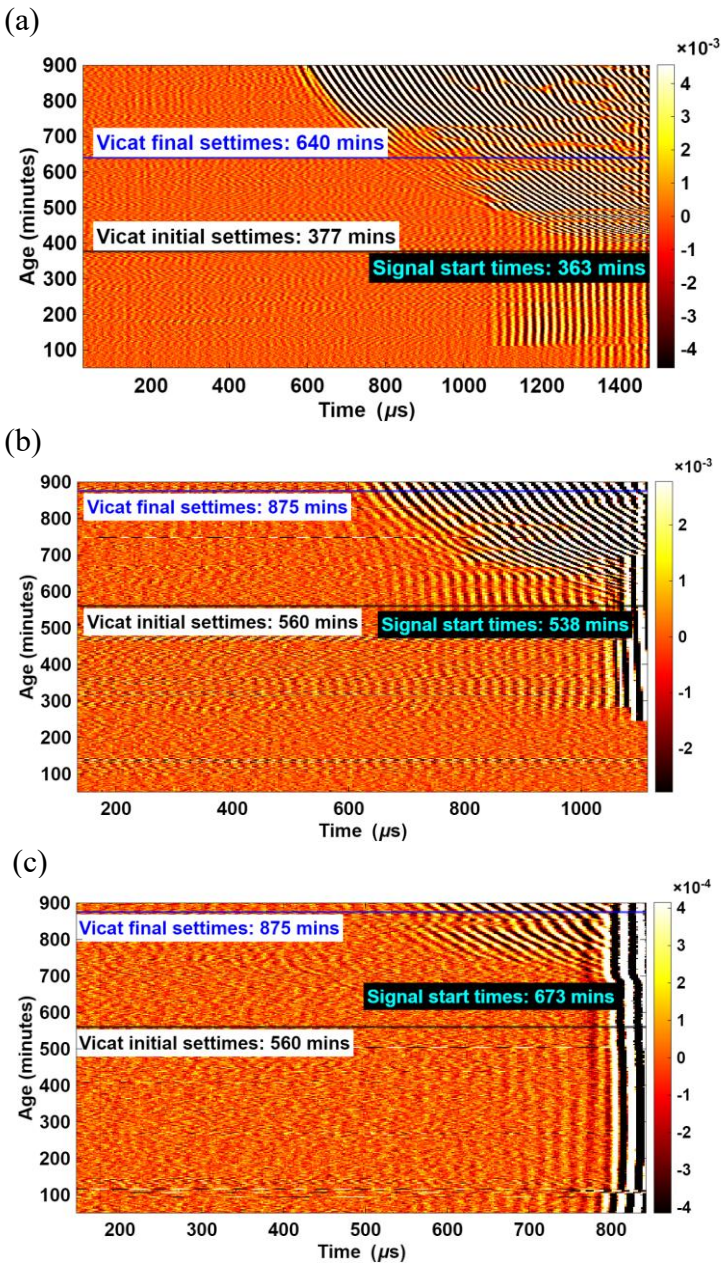

Figure 3. 2D heatmap of LR wave at incident angles of (a) 20 degrees; (b) 25 degrees; (c) 30 degrees. The plot captures time of LR wave propagation (μs) on the horizontal axis and material aging time (minutes) on the vertical axis, with a color bar indicating signal amplitude.

2. Correlation of nUT measurements with standard Vicat set times

Figure 4 presents 2D heatmap plots monitoring the development of LR wave signals at an incident angle of 20º for six cement paste mixtures with varying binder types and w/c ratios. Across all the six mixtures, the LR wave occurs earlier than, or close to, the standard Vicat initial set times. For the 100OPC1L mixtures, a distinct LR wave packet becomes visible well before the initial Vicat set times. The 0.4 w/c ratio showing the earlier LR emergence (238 minutes) than the 0.50 w/c mixture (290 minutes) and more gradual LR evolution; this ordering is consistent with the longer initial set typically observed for mixtures with higher water content.

For the FA paste mixtures, both w/c levels display LR wave initiation at later ages than the corresponding plain OPC mixes (278 and 397 minutes of signal start times), and the LR signal appears much earlier than the Vicat initial set times line, reflecting the retarded setting behavior commonly reported for fly ash–blended systems[27].

For the LC3 mixtures, the LR wave signal appears nearly at the Vicat initial set time, indicating that LC3 binders develop measurable stiffness sooner than FA binary mixtures with similar w/c[28]. The signal start time of w/c 0.4 and 0.5 are 316 and 363 minutes, while the Vicat initial set times are 320 and 377 minutes, respectively. A steeper LR trajectory indicates a faster velocity increase, so mixtures where the LR band quickly bends left suggest more rapid modulus development. The steepness of the LR trajectory makes the wavefield plot a quantitative "fingerprint" of how quickly the concrete is stiffening. It may control the construction schedule. For example, an assessment is optimal for sawcut timing of contraction joints in concrete pavements.

Overall, the relative timing of the LR wave signal starts and the Vicat initial set confirms that the LR wave 2D heatmap is a continuous indicator of early-age behavior compared to the single-time Vicat penetration measurement. This means the plots can potentially show not only when the set time occurs but also how sharply or gradually each mixture transitions from fluid to solid.

Across all six mixtures, the heatmap results show a consistent ultrasonic signature associated with the material reaching its final set. As the final set time approaches, the LR wave becomes increasingly well-defined, with noticeable changes in both arrival time and amplitude. Specifically, the LR wave's arrival time shifts earlier and the signal amplitude increases indicating faster surface-wave propagation as the paste stiffens and gains rigidity.

For mixtures containing only OPC (Figures 4a and 4b), the LR wave transitions sharply near the Vicat final set time (450 and 675 minutes). A clear strengthening of the wavefront and earlier arrival are observed, consistent with rapid stiffness gain after initial set. The fly-ash blended mixtures (Figures 4c and 4d) exhibit later final set times (680 and 875 minutes), and the heatmaps show a more gradual improvement in LR wave coherence, reflecting the slower hydration kinetics of class F fly ash. In contrast, the LC3 mixtures (Figures 4e and 4f) demonstrate relatively early final set times (510 and 640 minutes), with strong and early forming LR wave signatures. These mixtures show a rapid increase in amplitude and a pronounced shift in arrival time, aligning with the known accelerating effect of calcined clay on early hydration[28]. Overall, these results indicate that, demonstrating the nUT can produce consistent and reliable results for the Vicat final setting time. This could involve using nUT as a supplementary test alongside the lab-based ASTM C403 penetration method, offering the benefit that wet sieving to eliminate coarse aggregates is not required.

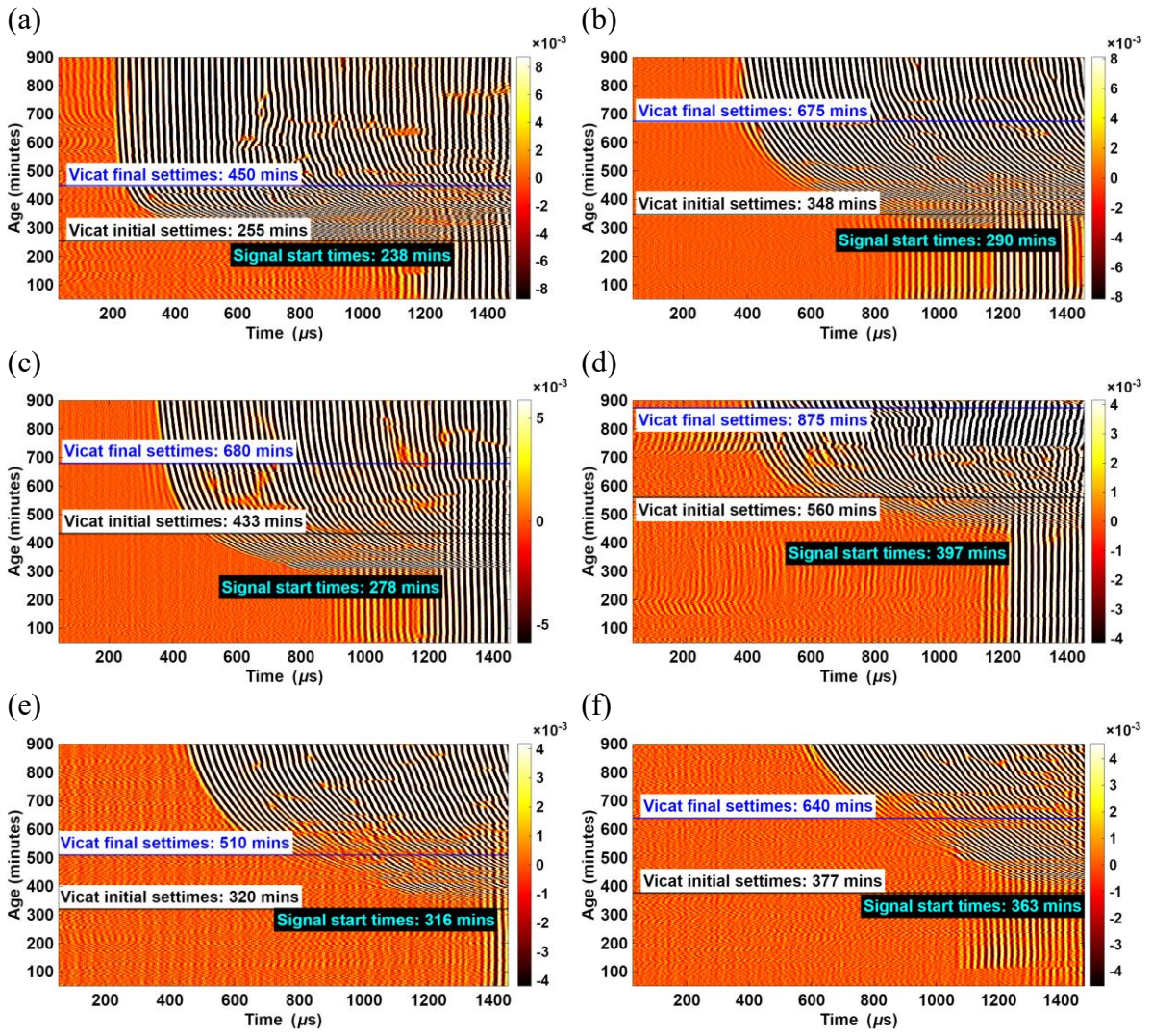

Figure 4. 2D heatmap of LR-wave at incident angle of 20 degrees of six paste mixtures (a) 100OPC1L-0.4; (b) 100OPC1L-0.5; (c) 70OPC1L:30FA-0.4; (d) 70OPC1L:30FA-05; (e) 100LC3-04; and (f) 100LC3-05

Table 2 presents the signal start times in minutes for six different mixtures, as recorded across 16 receivers. The mean initial set time varied from 244 to 427 minutes, with standard deviation varying from 4 to 22 minutes. The coefficient of variation (COV) between receivers at the same location was between 1 and 5%, demonstrating the nUT can produce consistent and reliable results for the initial setting time. It shows that all 16 receivers can detect earlier or very close to Vicat initial set time. Figure 5 shows that the signal start time of the mixtures

can be fairly estimated from the nUT based on the positive Pearson correlation of 78% between the standard Vicat initial set time and nUT.

Table 2. Signal start time (mins) of 6 mixtures at 16 sensors.

Receivers	100OPC1L-04	100OPC1L-05	70OPC1L:30FA-04	70OPC1L:30FA-05	100LC3-04	100LC3-05
1	248	299	288	397	316	374
2	250	292	284	421	318	372
3	242	288	276	458	318	363
4	248	293	284	416	318	379
5	245	295	290	416	321	374
6	248	289	287	424	319	380
7	244	292	294	425	310	378
8	244	288	281	413	318	373
9	242	294	291	468	321	372
10	246	291	275	413	320	377
11	242	297	289	420	321	384
12	243	288	271	413	322	375
13	242	292	277	478	322	373
14	236	303	305	414	353	412
15	238	297	270	426	321	377
16	240	290	278	425	323	371
Mean	244	293	284	427	321	377
Standard deviation	4	4	9	22	9	10
COV, %	2	1	3	5	3	3

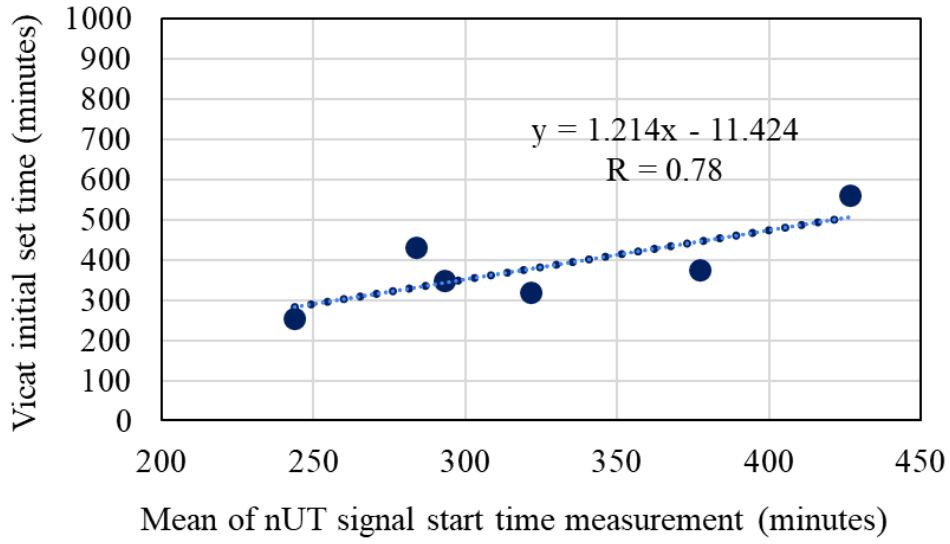

Figure 5. Relationship between Vicat initial setting time and nUT signal start time measurement

CONCLUSIONS

This study successfully developed and validated a fully non-contact ultrasonic technique (nUT) for the continuous, real-time determination of both initial and final setting times of cementitious materials, with a specific focus on emerging low-carbon binders. The portable and compact 12-hour battery life nUT system utilizes a 50 kHz ultrasonic transmitter to generate leaky Rayleigh (LR) waves on the cement paste surface, which are captured by 16 MEMs receivers' array without any mechanical coupling or embedded sensors. The key findings and implications of this research are as follows:

1. The nUT system reliably identified both intial and final set times by monitoring the emergence and evolution of LR wave signals. The initial of detectable LR wave energy correlated closely with the Vicat initial set times, while a well-defined increases in signal amplitude and a shift towards earlier arrival times corresponding to the Vicat final set time. This provides a continuous, quantitative fingerprint of the stiffening process, offering significant advantages over the single-point, intermittent measurement of standard methods.

2. Experimental results for six paste mixtures, incorporating OPC1L, LC3, and FA at w/c ratio of 0.4 and 0.5, demonstrated a strong correlation (Pearson R = 78%) between nUT measurements and Vicat test results. The signal start times (representing initial set across 16 receivers showed low coefficient of variation (1-5%), confirming the technique's reproducibility and consistency.

3. The research underscores the importance of incident angle optimization for exciting detectable LR waves across different hydration stages. 20 degrees of incidence angle shows the ability to detect stat signal time earlier compared to 25 and 30 degrees.

REFERENCES

1. Neville, A.M. and Brooks, J.J., "Concrete Technology". 2nd Edition, Pearson Education Ltd., London, 2010.
2. Zhang, Haimei, Shuo Ma and Yan-Min Wu., "Building materials in civil engineering: Chapter 5 - Concrete", Pages 81-149, 423, 2011.
3. Reynolds, C.E., Steedman, J.C., & Threlfall, A.J., "Reinforced Concrete Designer's Handbook (11th ed.)", CRC Press, 2007.
4. Tran, Q., and Roesler, J. R., "Noncontact Ultrasonic and Computer Vision Assessment for Sawcut Initiation Time," *Journal of Transportation Engineering*, Part B: Pavements, V. 146, No. 3, 2020, p. 04020055. doi: 10.1061/JPEODX.0000207.
5. Rahman M, Rawat S, Yang R (Chunhui), Mahil A, Zhang YX, "A comprehensive review on fresh and rheological properties of 3D printable cementitious composites", *Journal of Building Engineering*, 91:109719, 2024.
6. ASTM C191-21, "Test Methods for Time of Setting of Hydraulic Cement by Vicat Needle," ASTM International, West Conshohocken, PA, 2021.
7. ASTM C403-15, "Standard Test Method for Time of Setting of Concrete Mixtures by Penetration Resistance," ASTM International, West Conshohocken, PA, 2015.
8. Hermawan H, Zul Fahmi FR, "A state-of-the-art approach for the direct and indirect measurements of the ultrasonic wave reflection on the fresh cement paste in determining the setting behavior via Fourier transformations", *Journal of Building Engineering*, 106:112671.

9. Chung, C.-W.; Suraneni, P.; Popovics, J. S.; and Struble, L. J., "Setting Time Measurement Using Ultrasonic Wave Reflection," *ACI Materials Journal*, V. 109, No. 1, Jan.-Feb. 2012, pp. 109-118.
10. Yim HJ, Kim JH, Shah SP., "Ultrasonic monitoring of the setting of cement-based materials: Frequency dependence", *Construction and Building Materials*, 2014 Aug 29;65:518-525. doi: 10.1016/j.conbuildmat.2014.04.128.
11. Thomas Voigt and Yilmaz Akkaya and Surendra P. Shah., "Determination of Early Age Mortar and Concrete Strength by Ultrasonic Wave Reflections", *Journal of Materials in Civil Engineering*, 2003.
12. Zhang, W., Wu, F. & Zhang, Y, "Early Hydration and Setting Process of Fly Ash-blended Cement Paste under Different Curing Temperatures", J. Wuhan Univ. Technol.-Mat. Sci. Edit. 35, 551–560, 2020.
13. Chen, W., Shui, Z. & Li, Y, "Early age hydration of cement paste monitored with ultrasonic velocity and numerical simulation" *J. Wuhan Univ. Technol.-Mat. Sci. Edit.* 25, 704–707, 2010.
14. Zhang, Yunsheng & Zhang, Wenhua & She, Wei & Ma, Liguo & Zhu, Weiwei, "Ultrasound monitoring of setting and hardening process of ultra-high performance cementitious materials", Ndt & E International - NDT E INT. 47. 10.1016/j.ndteint.2009.10.006, 2009.
15. Benaicha M, Jalbaud O, Burtschell Y, "Ultrasonic characterization and mechanical performance of self-compacting concrete in fresh and hardened states" Ultrasonics. Aug;152:107657. doi: 10.1016/j.ultras.2025.107657, Epub 2025 Apr 4, PMID: 40199045.
16. Sharma, Shruti & Mukherjee, Abhijit, "Monitoring freshly poured concrete using ultrasonic waves guided through reinforcing bars", *Cement and Concrete Composites*, 55. 10.1016/j.cemconcomp.2014.09.011, 2015.
17. Tran, Q., & Roesler, J., "Contactless Ultrasonic Test System for Set Times of Mortar and Concrete", *ACI Materials Journal*, 118(2), 97–106, 2021.
18. Baral, Aniruddha & Roesler, Jeffery, "Early Age Monitoring of High Cement Replacement Mixtures for Pavement", *Transportation Research Record: Journal of the Transportation Research Board*, 2677, 2022.

19. Bai, Yunshan and Liu, Yuanxue and Gao, Guangjian and Cui, Dandan, “Estimating the Azimuth of Ae Source in Concrete Plate-Like Structures Using a Non-Contact Sensor Unit”, Available at SSRN: https://ssrn.com/abstract=4411816 or http://dx.doi.org/10.2139/ssrn.4411816, 2023.
20. Stein, Seth and Michael E. Wysession., “An Introduction to Seismology, Earthquakes, and Earth Structure.”, 2002.
21. J. D. Achenbach, “Wave Propagation in Elastic Solids”, 1st Edition, January 21, 2016.
22. Neuenschwander, J.; Schmidt, T.; Lüthi, T.; and Romer, M., “Leaky Rayleigh Wave Investigation on Mortar Samples,” Ultrasonics, V. 45, No. 1-4, 2006, pp. 50-55. doi: 10.1016/j.ultras.2006.06.002.
23. Choi, H., Song, H., Tran, Q. N. V., Roesler, J. R., & Popovics, J. S., “Contactless System for Continuous Monitoring of Early-Age Concrete Properties”, Concrete International, 38(9), 35–35, 2016.
24. Tran, Q., “Noncontact sensing systems and autonomous decision-making for early-age concrete”, Dissertation, University of Illinois at Urbana-Champaign, 2020-03-16.
25. Wang KJ, Kwon SJ, Wang XY, “Optimal mixture design method for low-CO2 limestone-calcined clay cement (LC3) concrete considering climate change and carbonation durability: A case study of eight countries”, Sustain Chem Pharm 46:102108, 2025.
26. Hosen K, Chen B, “Limestone calcined clay cement (LC3): A review of materials, properties, production and environmental impact”, *Journal of Building Engineering*, 112:113672, 2025.
27. Eren, O., Brooks, J. J., and Celik, T., "Setting Times of Fly Ash and Slag-Cement Concretes as Affected by Curing Temperature," Cement, Concrete, and Aggregates, CCAGDP, Vol. 17, No. 1, June 1995, pp. 11-17.
28. Ghazy MF, Maaty ESA, Elaty MA, Rwashdeh AA Al, “A Comprehensive Review of Limestone Calcined Clay Cement (LC3): Environmental and Properties Benefits, Challenges, Opportunities, and Future Directions”, Results in Engineering 108319, 2025.